

VESSEL IMPACT ANALYSIS FOR RISER PROTECTION FRAME AND PROTECTION NET SUPPORTS ON SEMI-SUBMERSIBLE OFFSHORE STRUCTURES

Özgür ÖZGÜÇ*

**INPEX Exploration and Production, South Korea*

ABSTRACT

The objective of this paper is to assess the collision strength of the riser protection frame (RPF) and protection net (PN) supports of CPF (Central Processing Facility) of Semi-Submersible types. The RPF and PN supports are assessed for their collision strength when they are being collided by a supply vessel. The vessel colliding from north-side is assumed to be 18,000 tons and the one colliding from east/west side is assumed to be 7000 tons. The focus of this paper is placed on general methodology and design of accident scenarios for CPF using more sophisticated tools such as the non-linear FEM which predicts the structural responses during and after a collision more precisely. There are two different designs for the RPF and PN supports and thus there are four structures i.e. RPF-01, RPF-02, PN-01 and PN-02. The expected kinetic energy for the collision from the north side is 20MJ. The collision energy from east/west side is 14MJ for side collision and 11MJ for bow/stern collision. With collision energy and plastic strain criteria, the collision capacities of the RPF and PN supports are estimated along the span of the structures for the given collision energies.

Keywords: Collision, Accident scenarios, Non-linear FEM, Riser Protection Frame (RPF), Protection Net (PN)

1. Introduction

There are some limited reports on ship-to-platform collision and the consequential risks to the damaged structures. Experts recognize that ship collisions are not likely to cause the push-over failure of collided platforms that lose some individual structural members, especially in a benign environment. However, minimum structures may see rapid deterioration of the overall structural integrity if impact damages are left unrepaired [2].

Vessel collision during normal operations is one of the accidental loading possibilities. Such a scenario for platforms in the Gulf of Mexico is possible when 1,000-ton supply vessel collides, either head-on or broadside, with the platform at a speed of 0.5 m/s. The vessel is chosen to represent typical OSVs in the U.S. Gulf of Mexico [4, 5]. This API RP [1] requires that the platform survive the initial collision, and meet the post-impact criteria. During the described collision, the offshore structure absorbs energy primarily from localized plastic deformation of the tubular wall, elastic/plastic bending, and elongation of the member. In addition, if the fendering device is fitted, then there is global platform deformation, in addition to ship deformation and/or rotation. After collision, the damaged platform should retain sufficient residual strength to withstand environmental storm loads for one-year in addition to normal

operation loads. In the North Sea (see, e.g., ISO 2005a), the collision is described as one from a vessel of 5,000 tons with a drifting speed of 2.0 m/s. The collision energy is 14 MJ for a broad-side collision and 11 MJ for a head-on collision [3, 7].

In an analysis of a collision between a supply vessel and an FPSO in West Africa, Oh et al [10] assumed that a collision could occur in three places: on the riser, the protector, and the deflector. They selected to look into collisions that induce large deformations on the framed structure at a colliding speed of 1 m/s. They estimated that the speed was a result of marine equipment failure, or human error.

Lin et al [6] showed how FEM is used to simulate the collision process of two semi submersibles. Stress and strain distributions, collision forces, and plastic energy absorption are obtained. The motion lag of the struck submersible in the collision process is discussed and it is found that it is sensitive to impact velocity which increases with the increasing velocity.

The objective of this analysis is to assess the collision strength of the riser protection frame (RPF) and protection net (PN) supports of Ichthys Inpex CPF. The riser protection frame and protection net supports are assessed for their collision strength when they are being collided by a supply vessel. The colliding vessel from north-side is assumed to be of 18,000 tons and from east/west side it is 7000 tons.

The finite element model is developed using MSC/PATRAN and analysis is performed in LS-DYNA. The element size used in the FE model is one-longitudinal spacing away from the concerned location. In the concerned location it is 100mm× 100mm. In the concerned location only shell elements are used. There are two different designs for the RPF and PN supports and thus there are four structures i.e. RPF-01, RPF-02, PN-01 and PN-02. The expected kinetic energy for the collision from the north side is 20MJ. The collision energy from east/west side is 14MJ for side collision and 11MJ for bow/stern collision.

The material assumed is EW420 which has a minimum yield strength of 380MPa and a tensile strength of 530MPa. Initially the collision analysis is performed with an objective of achieving zero plastic strain on the CPF column structure that is supporting the RPF and PN supports, but later it is realized that practically it is not possible to achieve no plastic strain for the given collision energy. Hence a plastic strain of 5% on the outer shell of the CPF column structure is assumed to be acceptable. Since the final objective is to check any kind of leakage into the CPF column due to the collision, it is important to control the plastic strain on the outer shell of the column. Since the plastic strain of the internal members of the column, RPF and PN structures, doesn't cause any leakage inside the column, it is proposed to have no criterion for the plastic strain of these structural members [8, 9].

Thus with the above collision energy and plastic strain criteria, the collision capacities of the/-RPF and PN supports are estimated along the span of the structures for the given collision energies.

2. Project Description

In 1998, INPEX Exploration and Production acquired the petroleum exploration permit WA-285-P, located in the Browse Basin, off the north-west coast of Western Australia and

approximately 820 kilometers south-west of Darwin. During 2000 to 2001, three exploratory wells resulted in the discovery of an extremely promising gas and condensate field now known as the Ichthys Field. The field was named after the classical Greek word for “fish”. Most likely resource estimates are 12.8 trillion cubic feet of gas and 527 million barrels of condensate to be produced over an operational life of more than 40 years.

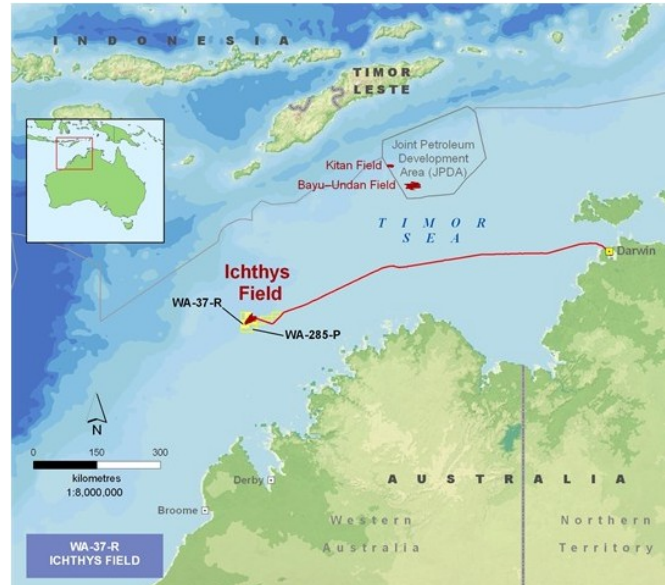


Figure 1. Project field location

Gas from the Ichthys Field will undergo preliminary processing at the offshore central processing facility (CPF) to remove water and raw liquids, including a large proportion of the condensate. This condensate will be pumped to a floating production, storage and offloading (FPSO) facility anchored nearby, from which it will be transferred to tankers for delivery to markets. These FPSO facilities include mercury removal from condensate, flash gas compression, MEG regeneration / reclamation and produced water treatment facilities.

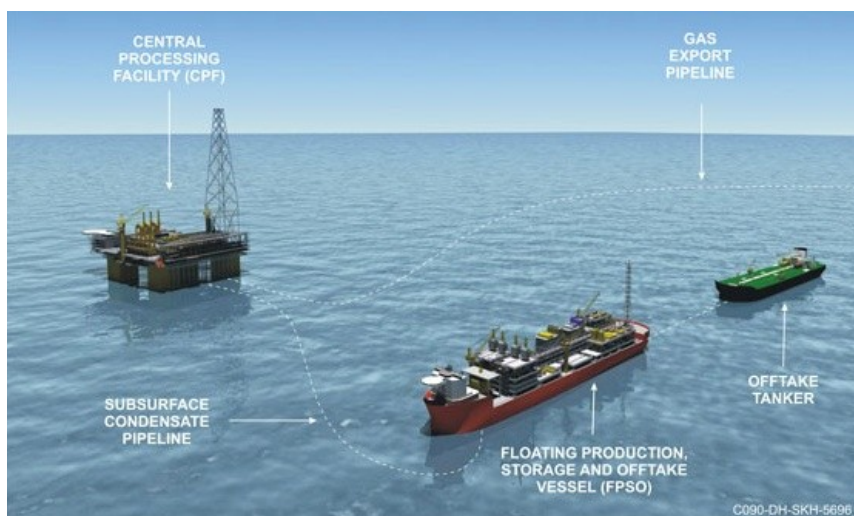


Figure 2. Offshore facilities layout

3. CPF Design

The CPF is a column-stabilized, offshore semi-submersible production unit supporting hydrocarbon processing systems and utilities, as well as living quarters for about 200 people.

INPEX's CPF will be the world's largest semi-submersible platform. It is being constructed in South Korea at the Samsung Heavy Industries shipyard.

Once constructed, the facility will be towed about 6,000 kilometers to the Ichthys Field in the Browse Basin, offshore Western Australia. It will be permanently moored near the Field for the life of the Project by 28 mooring lines, representing more than 25,000 tons of anchor chain.

The main dimensions on the hull are given from Table 1 to Table 3 as follows.

Table 1. Main Dimensions – General

Operation draught (from keel)	26.00 m
Height, keel to underside Toppides BOS	48.00 m
Height, keel to main deck, TOS	62.00 m
Hull outer dimension excluding Guide Tube Box	110.30 m
Hull outer dimension incl. Guide Tube Box	118.675 m
Column spacing (center to center), (longitudinal and transverse)	83.65 x 83.65 m

Table 2. Main Dimensions – Pontoon (rectangular ring)

Breadth	26.65 m
Height	11.875 m
Bilge radius	1.25 m
Breadth, Guide Tube Box	8.375 m
Height, Guide Tube Box	5.22/6.25 m
Length, Guide Tube Box	103.00 m

Table 3. Main Dimensions – Columns (rectangular types)

Number of columns	4
Width	26.65 m
Corner radius	6.20 m
Height from keel to top of column	48.00 m

A computerized hull structural and finite element (FE) models are demonstrated on Figure 3 and Figure 4.

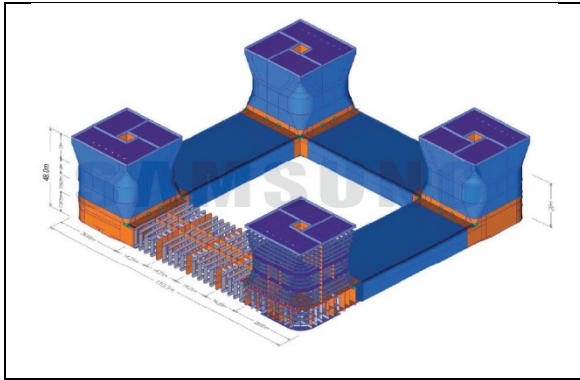


Figure 3. Hull Main Dimensions

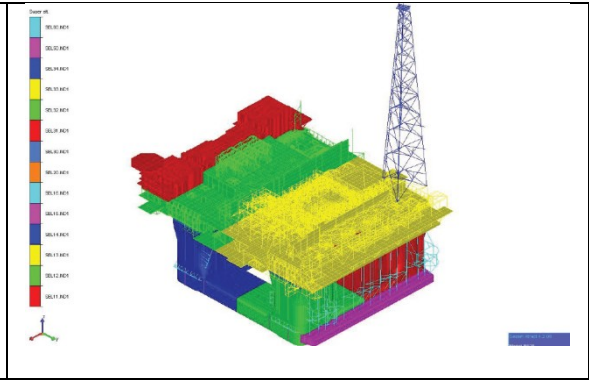


Figure 4. Computer FE model

3.1 Layout Details

Layout details and relevant drawings of RPF and PN structures of CPF are shown from Figure 5 to Figure 9.

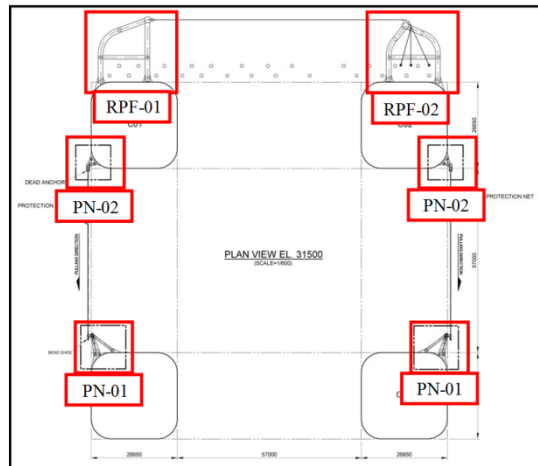


Figure 5. Layout of CPF showing the RPF and PN structure

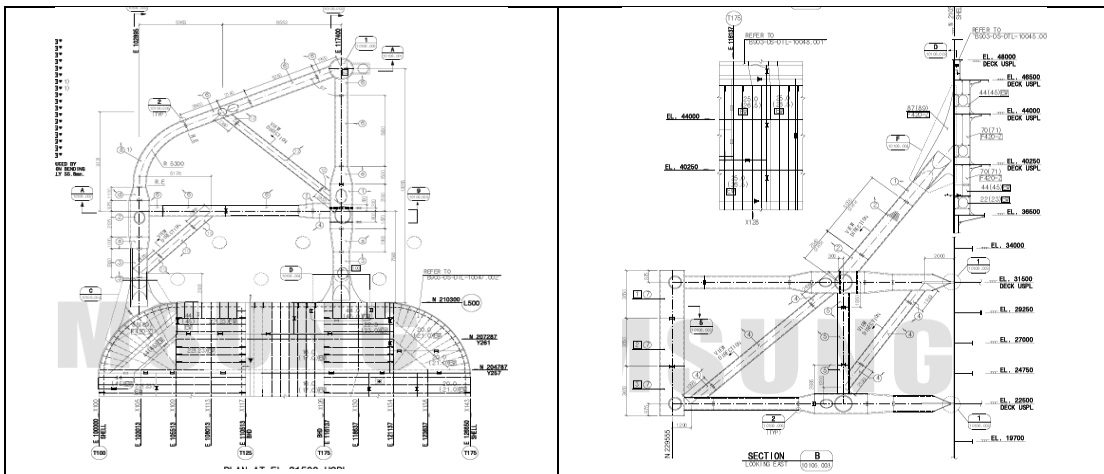


Figure 6. Drawing of RPF-01 of CPF

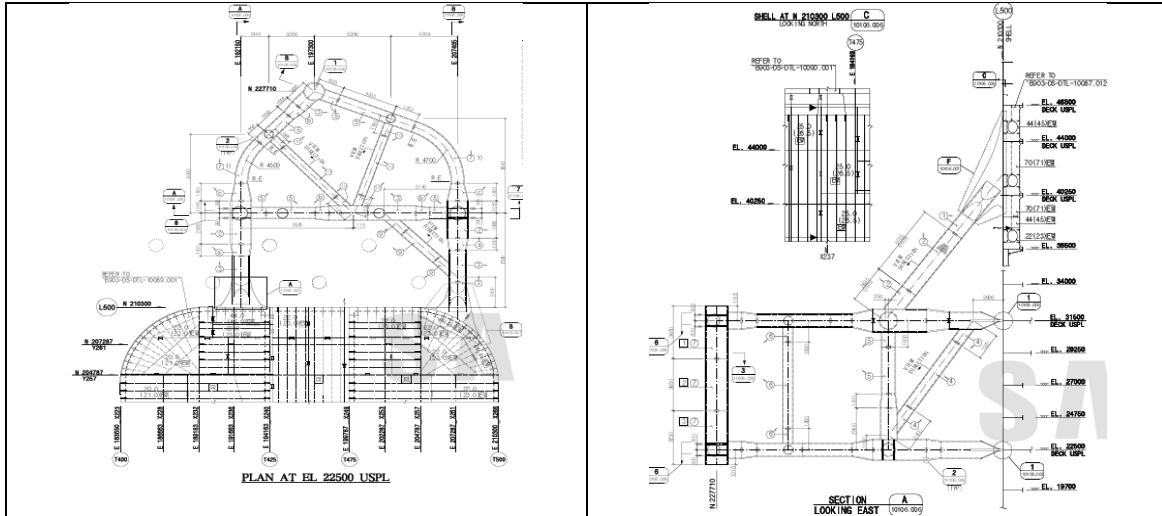


Figure 7. Drawing of RPF-02 of CPF

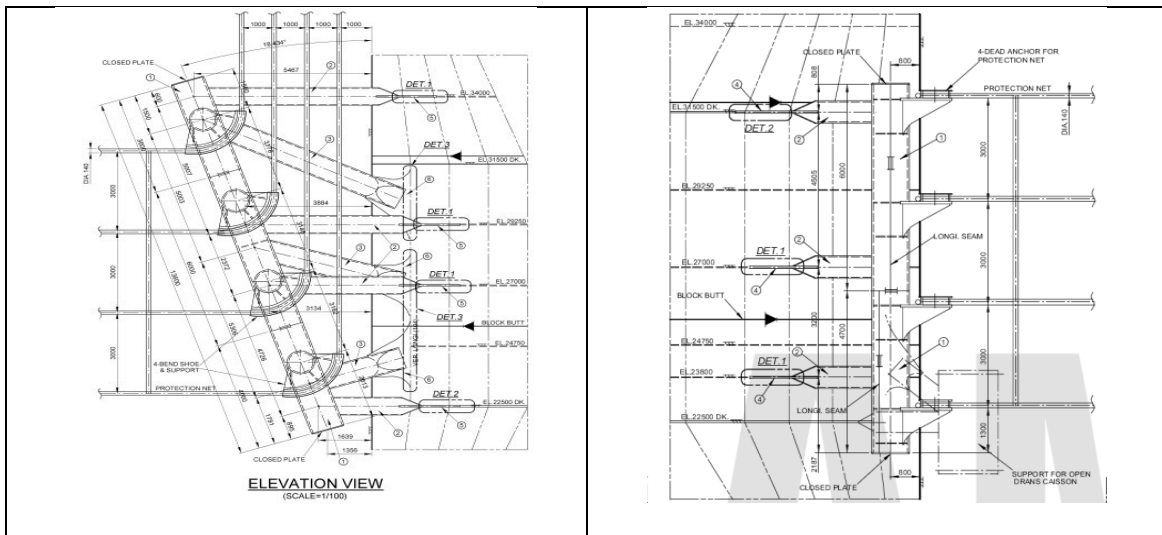


Figure 8. Drawing of PN-01 of CPF

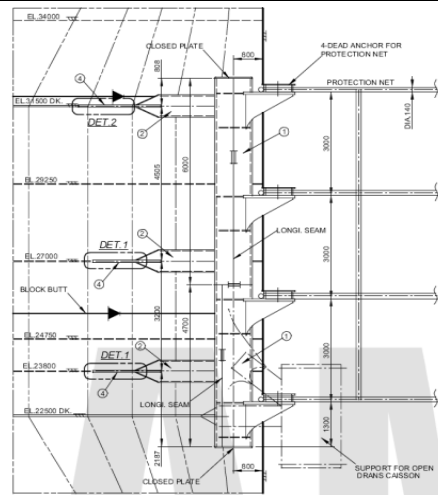


Figure 9. Drawing of PN-02 of CPF

4. FE Model

Figures 10 ~ 13 show the FE models of the RPF and PN supports of CPF. The finite element model is developed using MSC/PATRAN and analysis is performed in LS-DYNA. The element size used in the FE model is one-longitudinal spacing away from the concerned location. In the concerned location it is 100mm× 100mm. In the concerned location only 2-D shell elements are used where as in the other locations both 1-D bar elements and 2-D shell elements are use [11].

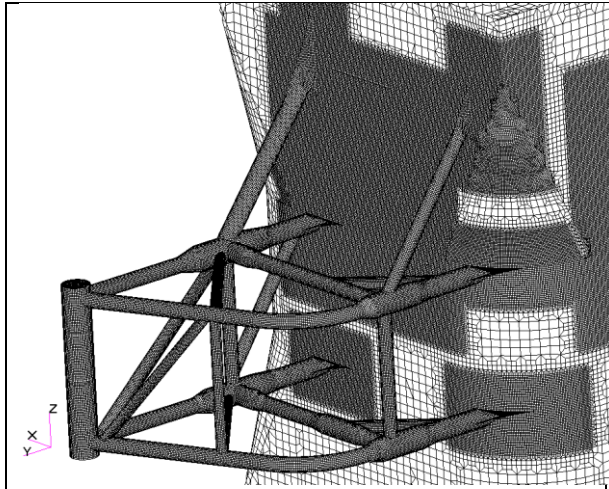


Figure 10. FE model of RPF-01 of CPF

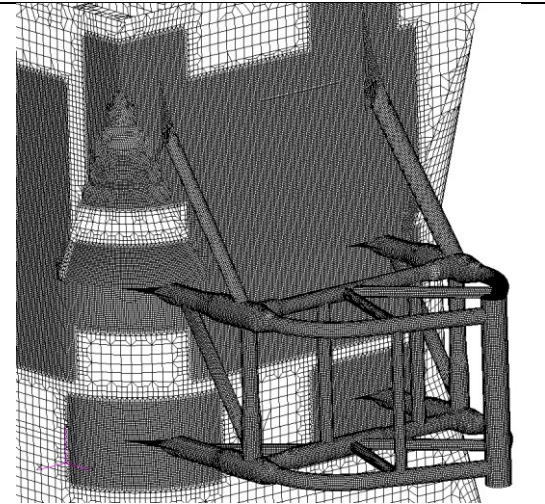


Figure 11. FE model of RPF-02 of CPF

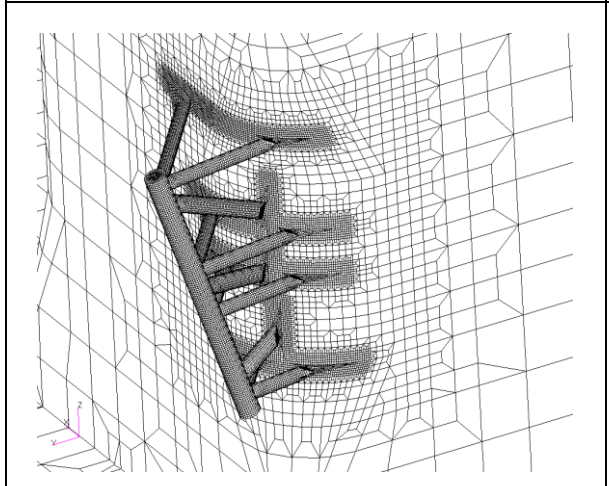


Figure 12. FE Model of PN-01 of CPF

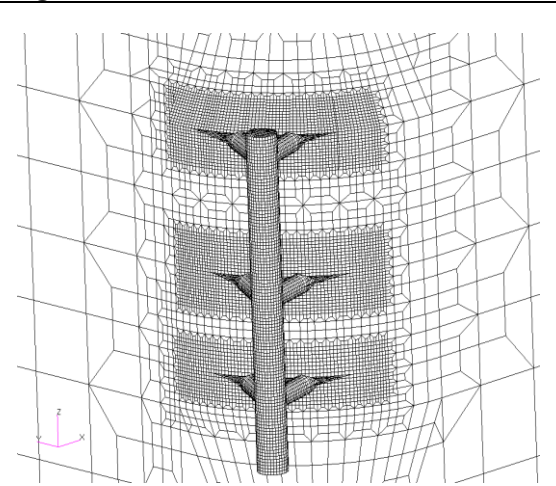


Figure 13. FE Model of PN-02 of CPF

4.1. Material Properties and Allowable Criteria

The material properties assumed in the present analysis is EW420 and its properties are given in Table 3.1.

Table 4. Material properties of EW420

Young's modulus, E, MPa	Poisson's ratio, ν	Density, Kg/m ³	Yield strength MPa	Tensile strength MPa
$2,05 \times 10^5$	0,3	7850	380	530

Material nonlinearity i.e. PIECEWISE LINEAR PLASTIC property as defined in the

material library of LS-DYNA is defined for the RPF, PN supports and the CPF Column structure. The striking vessel is assumed to be rigid and thus RIGID property as defined in the material library of LS-DYNA is defined for the striking vessel.

By assuming the striking vessel to be rigid, the colliding energy of the striking vessel is completely transferred to the struck vessel i.e. RPF support, PN support and the CPF

Column structure, thus the results obtained with this assumption is conservative. Initially the collision analysis is performed with an objective of achieving zero plastic strain on the CPF column structure that is supporting the RPF and PN supports but later it is realized that it is practically not possible to design the structures with no plastic strain for the given colliding energies. Hence a plastic strain of 5% on the outer shell of the CPF column structure is assumed to be acceptable. Since the final objective is to check any kind of leakage into the CPF column due to the collision, it is important to control the plastic strain on the outer shell of the column. Since the plastic strain of the internal members of the column, RPF and PN structures, doesn't cause any leakage inside the column, there is no criterion for the plastic strain of these structural members.

4.2. Loads and Boundary Conditions

The expected kinetic energy for the collision from the north side is 20MJ. The collision energy from east/west side is 14MJ for side collision and 11MJ for bow/stern collision.

To check whether the collision simulations are carried out properly, both the kinetic energy of the striking vessel and the absorbed internal energy of FPSO hull structure are plotted based on time history. It is confirmed that for the all cases the kinetic energy starts from the required energy level and the internal energy is exactly same as initial kinetic energy level of striking vessel. From the analysis results summarized below, it is proven that the collision loadings are properly applied and the simulations are carried out reasonably.

For the collision from north-side:

Mass of supply vessel is 18,000 tons and the expected collision energy from north side is 20MJ. By considering the DNV rules (DNV-OS-A101), the added mass is taken into account and thus the required velocity of the striking vessel is calculated so as to obtain the kinetic energy of 20MJ on the striking vessel.

For the collision from east/west side:

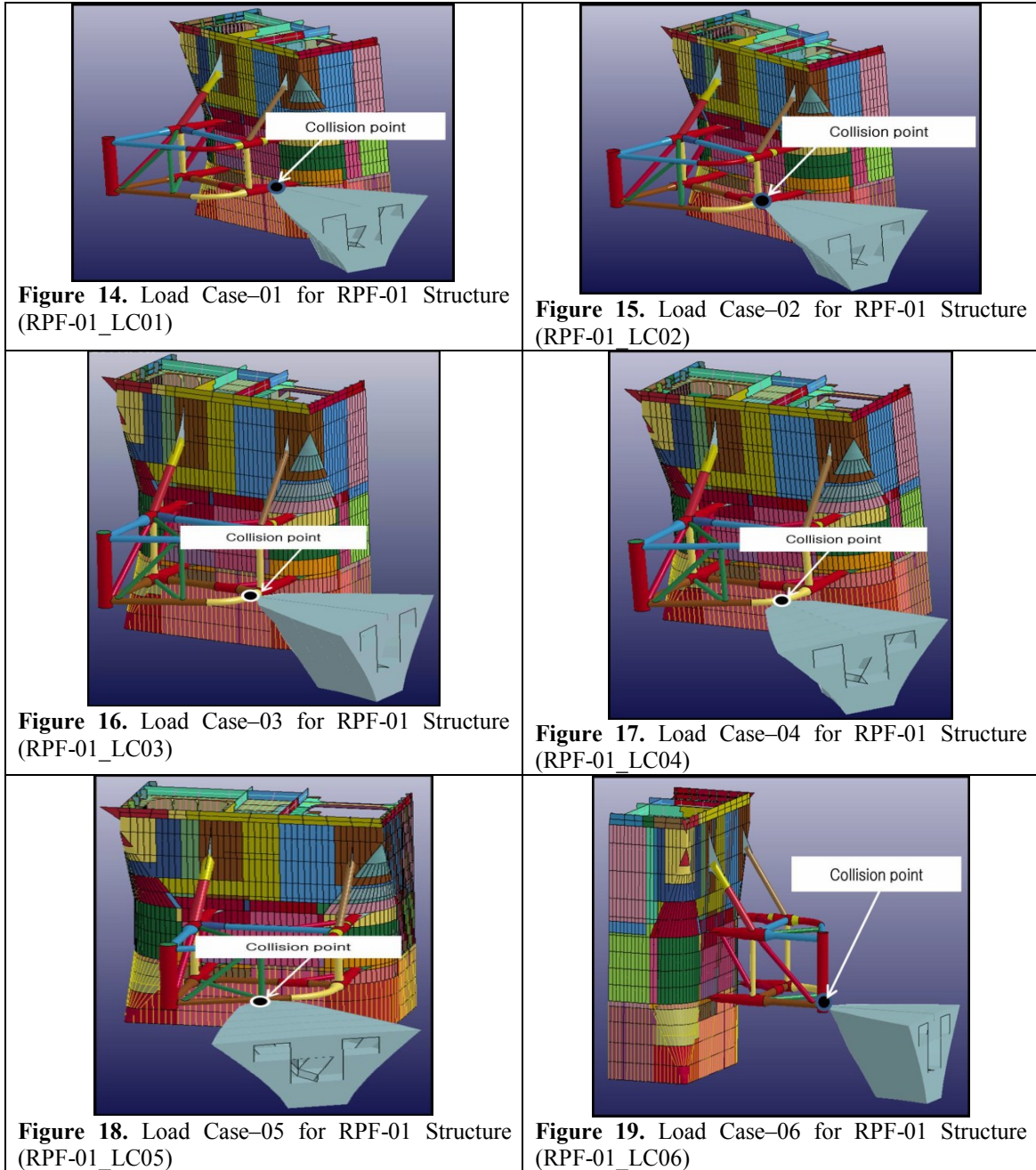
The mass of the striking vessel from east/west side is 7,000tons. The kinetic energy for collision from east/west side is 14MJ (for side collision) and 11MJ (for bow/stern collision) as per DNV-OS-A101.

The boundary conditions on the FE model are appropriately given to constrain any kind of rigid body motion.

Load Cases:

The collision capacities of the RPF and PN supports are estimated along the span of these structures and hence different load cases are considered for each structure, in which each load case defines the collision scenario at different points of collision. Figure 14~24 show

different load cases on RPF-01 and RPF-02 supports at different points of collision. Figure 25 ~ 36 show different load cases on PN-01 and PN-02 supports at different points of collision.



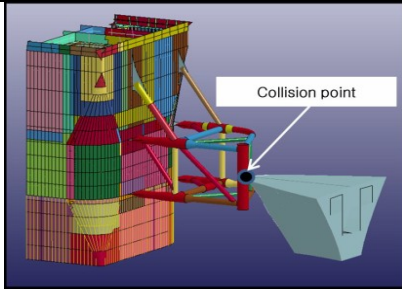


Figure 20. Load Case-07 for RPF-01 Structure (RPF-01_LC07)

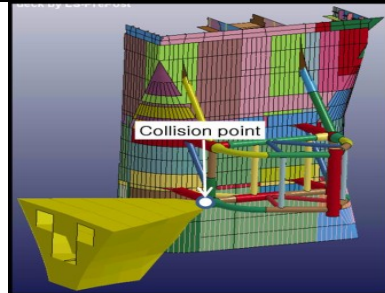


Figure 21. Load Case-02 for RPF-02 Structure (RPF-02_LC02)

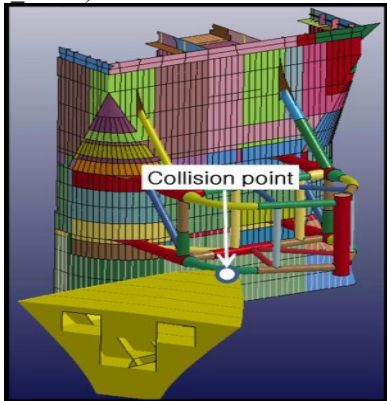


Figure 22. Load Case-03 for RPF-02 Structure (RPF-02_LC03)

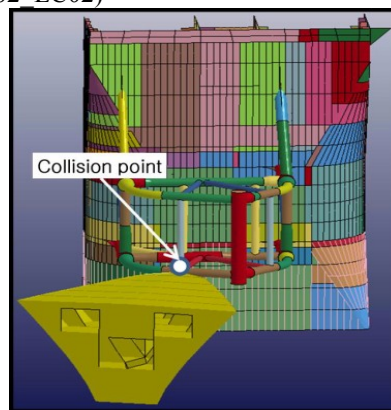


Figure 23. Load Case-04 for RPF-02 Structure (RPF-02_LC04)

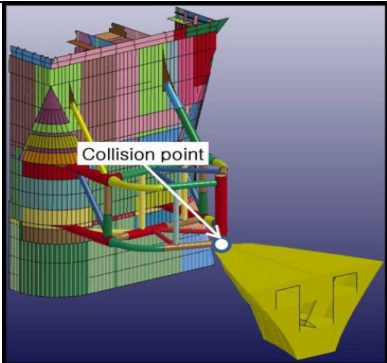


Figure 24. Load Case-05 for RPF-02 Structure (RPF-02_LC05)

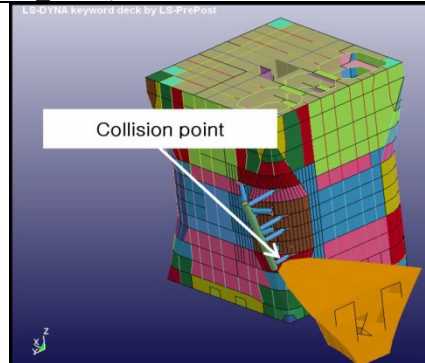


Figure 25. Load Case-01 for PN-01 Structure (PN-01_LC01)

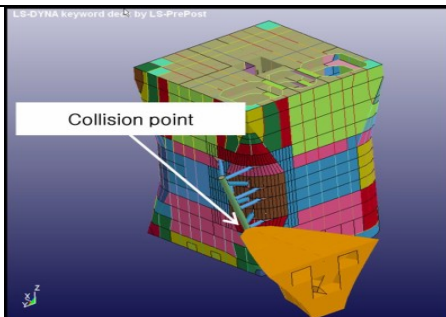


Figure 26. Load Case-02 for PN-01 Structure (PN-01_LC02)

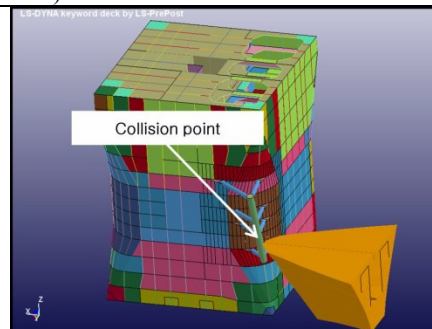


Figure 27. Load Case-03 for PN-01 Structure (PN-01_LC03)

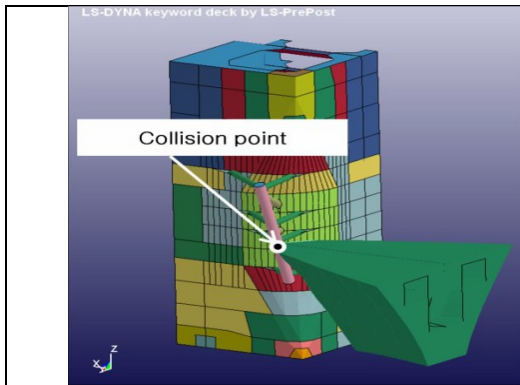


Figure 28. Load Case-04 for PN-01 Structure (PN-01_LC04)

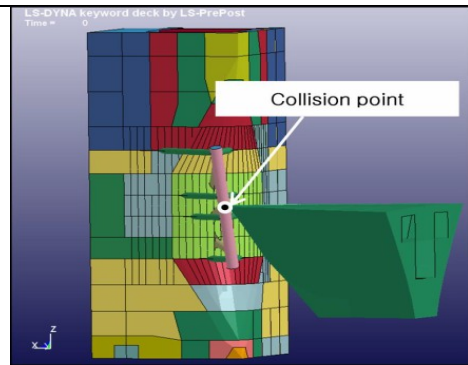


Figure 29. Load Case-05 for PN-01 Structure (PN-01_LC05)

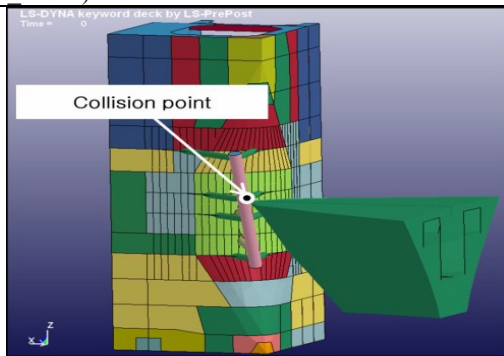


Figure 30. Load Case-06 for PN-01 Structure (PN-01_LC06)

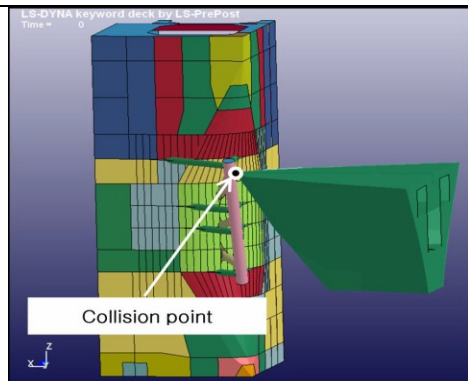


Figure 31. Load Case-07 for PN-01 Structure (PN-01_LC07)

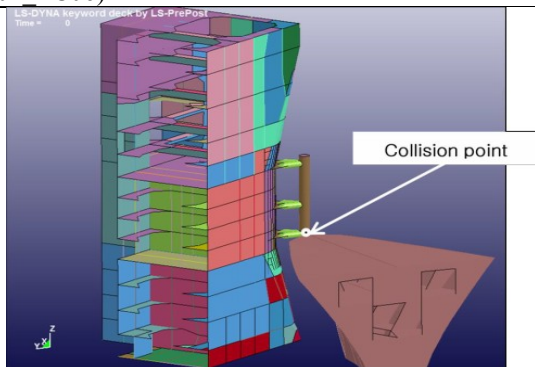


Figure 32. Load Case-01 for PN-02 Structure (PN-02_LC01)

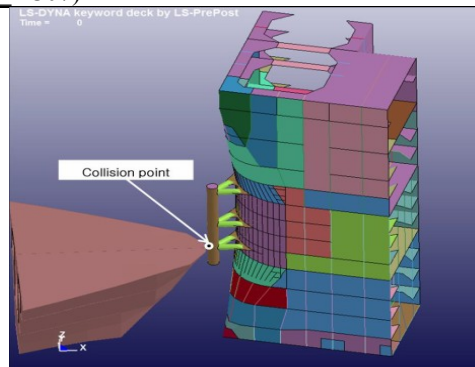


Figure 33. Load Case-02 for PN-02 Structure (PN-02_LC02)

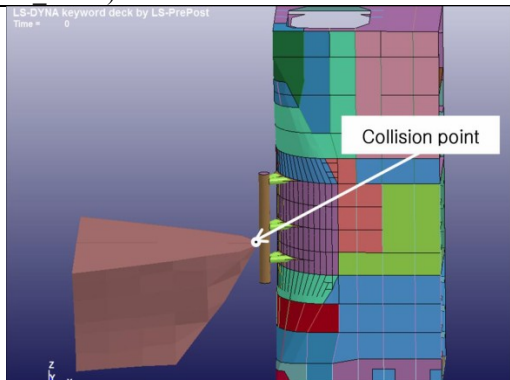
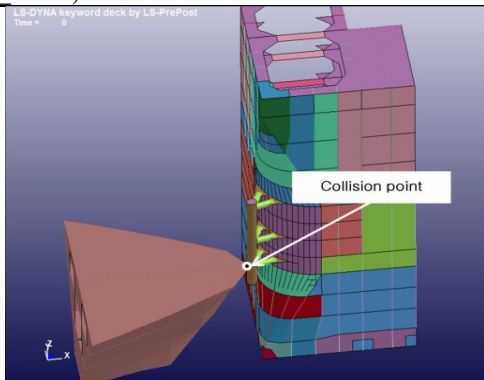
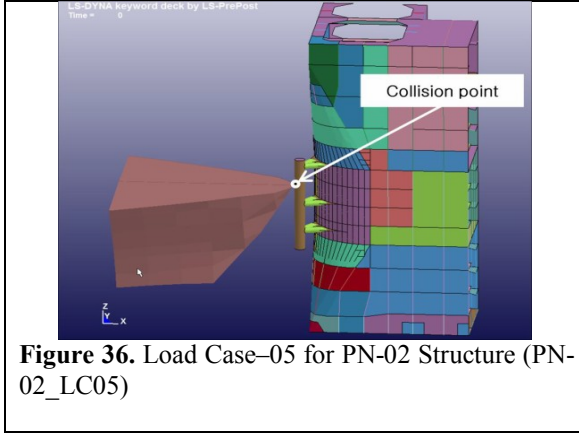


Figure 34. Load Case-03 for PN-02 Structure (PN-02_LC03)**Figure 36.** Load Case-05 for PN-02 Structure (PN-02_LC05)**Figure 35.** Load Case-04 for PN-02 Structure (PN-02_LC04)**Table 5.** Load cases of RPF and PN Structures.

Structure	Load Cases	Load Cases	Load Cases
RPF-01	RPF-01_LC01	RPF-01_LC02	RPF-01_LC03
	RPF-01_LC04	RPF-01_LC05	RPF-01_LC06
	RPF-01_LC07		
RPF-02	RPF-02_LC01	RPF-02_LC02	RPF-02_LC03
	RPF-02_LC04	RPF-02_LC05	
PN-01	PN-01_LC01	PN-01_LC02	PN-01_LC03
	PN-01_LC04	PN-01_LC05	PN-01_LC06
	PN-01_LC07		
PN-02	PN-02_LC01	PN-02_LC02	PN-02_LC03
	PN-02_LC04	PN-02_LC05	

It is to be noted that the colliding vessel is assumed to be completely rigid structure i.e. no absorption of any fraction of the collision energy. Thus the complete kinetic energy during collision is assumed to be absorbed by the RPF/PN supports and the CPF column only.

In all the collision scenarios, the collision is a point-contact and not line-contact, which gives conservative results. Thus it can be said that the obtained results are very conservative.

5. FE Collision Analysis Results

With described loads and boundary conditions collision analysis is performed for all the four structures by using LS-DYNA. Table 6 ~ 9 show the results of the collision analysis on RPF-

01, RPF-02, PN-01 and PN-02 structures, respectively.

Figures 37 ~ 40 show the plastic strain on the CPF column due to collisions at different points of the RPF and PN supports. Figures 41 ~ 46 show the displacements of the RPF and PN supports after collisions. Appendix B shows the capacities of the CPF column for collisions at different points of the RPF and PN supports. Figures 47 - 54 show the stress distribution plot of the CPF column due to collision at different points of the RPF and PN supports. Figures 55 ~ 62 show the strain distribution plot of the CPF column due to collision at different points of the RPF and PN supports.

Table 6. Results of the collision analysis of RPF-01 Structure

Load Case	Disp (mm)	% Plastic strain on	% Plastic strain on	Capacity (No plastic strain)
		Outer-shell – 20MJ	Outer-shell – 14MJ	
RPF-01_LC01	175 (14MJ)	-	4.5%	0 MJ
RPF-01_LC02	150 (14MJ)	-	0.5%	7 MJ
RPF-01_LC03	250 (20MJ)	0.25%	No strain	13 MJ
RPF-01_LC04	750 (20MJ)	No strain	No strain	20 MJ
RPF-01_LC05	400 (20MJ)	No strain	No strain	20 MJ
RPF-01_LC06	<50 (20MJ)	No strain	No strain	20 MJ
RPF-01_LC07	250 (20MJ)	No strain	No strain	20 MJ

The plastic strain for RPF-01_LC01 for 14MJ is 4.5%, since the point of collision is very close to CPF column. Appendix B shows the detailed graph from which the amount of colliding energy for 5% plastic strain can be obtained. It is to be noted that the load cases RPF-01_LC01~LC02 are the load cases where the collision points are very close to the CPF column and hence the collision capacities are very low i.e. less than 14MJ and hence the collision results for higher kinetic energy i.e. 20MJ is irrelevant and hence not calculated.

Table 7. Results of the collision analysis of RPF-02 Structure

Load Case	Disp. (mm)	% Plastic strain on	% Plastic strain on	Capacity (No plastic strain)
		Outer-shell – 20MJ	Outer-shell – 14MJ	
RPF-02_LC01	200 (20MJ)	3.90%	0.90%	0 MJ
RPF-02_LC02	185 (20MJ)	1.40%	0.65%	6 MJ
RPF-02_LC03	500 (20MJ)	No strain	No strain	20 MJ
RPF-02_LC04	590 (20MJ)	No strain	No strain	20 MJ
RPF-02_LC05	520 (20MJ)	No strain	No strain	20 MJ

The plastic strain for PN-01_LC01 for 14MJ is high (about 6.8%) since the point of collision is very close to CPF column. From the results it can be understood that the capacity of collision at this point is less than 14MJ and to achieve 0.0% plastic strain the energy should

not be more than 3MJ. Figures show the detailed graph from which the amount of colliding energy for 5% plastic strain can be obtained.

Table 8. Results of the collision analysis of PN-01 Structure

Load Case	Disp. (mm) (14MJ)	% Plastic strain on Outer-shell – 14MJ	% Plastic strain on Outer-shell – 11MJ	Capacity (No plastic strain)
PN-01_LC01	2000	6.8%	3.50%	3MJ
PN-01_LC02	1500	5.0%	3.75%	5MJ
PN-01_LC03	1350	3.5%	1.0%	1MJ
PN-01_LC04	520	1.6%	0.8%	4MJ
PN-01_LC05	700	1.2%	0.5%	7MJ
PN-01_LC06	700	2.5%	1.0%	9MJ
PN-01_LC07	1500	2.2%	1.2%	6MJ

Table 9. Results of the collision analysis of PN-02 Structure

Load Case	Disp. (mm) (14MJ)	% Plastic strain on Outer-shell – 14MJ	% Plastic strain on Outer-shell – 11MJ	Capacity (No plastic strain)
PN-02_LC01	1000	No strain	No strain	11MJ
PN-02_LC02	200	No strain	No strain	11MJ
PN-02_LC03	180	No strain	No strain	11MJ
PN-02_LC04	420	1.15%	0.26%	8MJ
PN-02_LC05	800	No strain	No strain	11MJ

Even though the plastic strain in the internal members of the CPF column is found to be high, it does not cause any leakage of the outer shell of the CPF column structure. It should also be noted that the present analysis is performed with an assumption that the total collision energy will be absorbed only by the struck vessel i.e. CPF column and the striking vessel doesn't take any amount of the collision energy, which is a very conservative approach. In practical situations there is always some percentage of energy which is absorbed by the striking vessel also and some percentage of energy is also released during collision of the striking and the struck vessels.

In practical situations a minimum of 40% of the colliding energy is expected to be absorbed by the striking vessel itself which can bring down the plastic strain of the internal members to much lower values. Hence it can be said that plastic strain of the internal members of the CPF

column will also drop down within the tolerable limits in the practical working conditions.

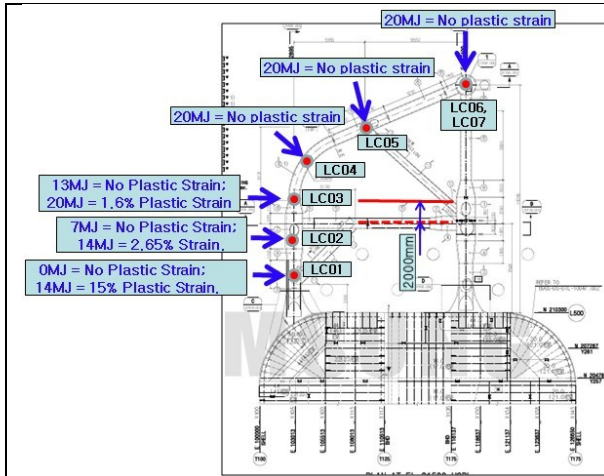


Figure 37. Collision capacity of RPF-01 w.r.t plastic strain on the CPF column

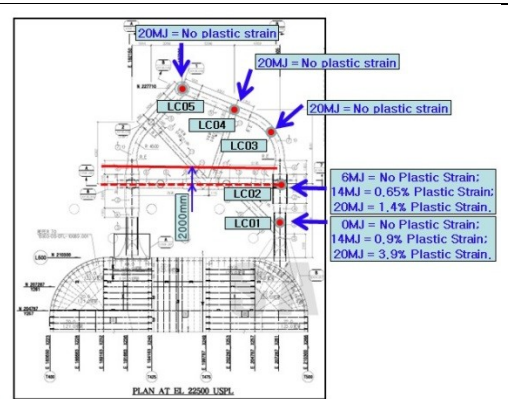


Figure 38. Collision capacity of RPF-02 w.r.t plastic strain on the CPF column

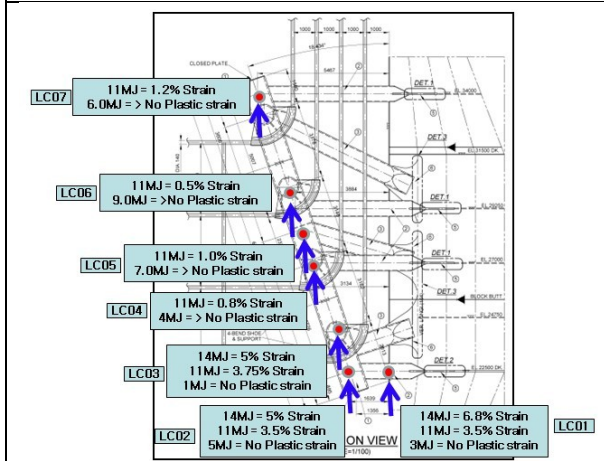


Figure 39. Collision capacity of PN-01 w.r.t plastic strain on the CPF column

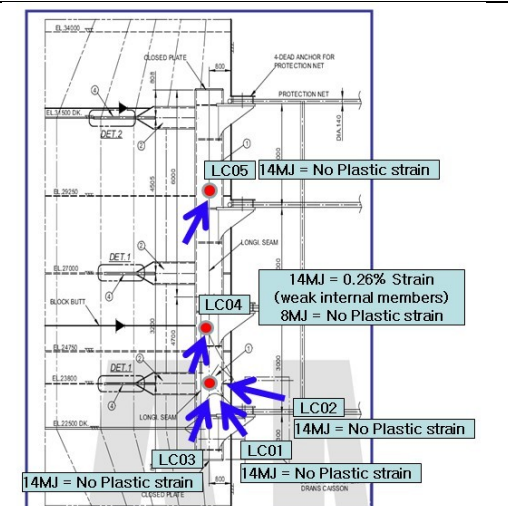


Figure 40. Collision capacity of PN-02 w.r.t plastic strain on the CPF column

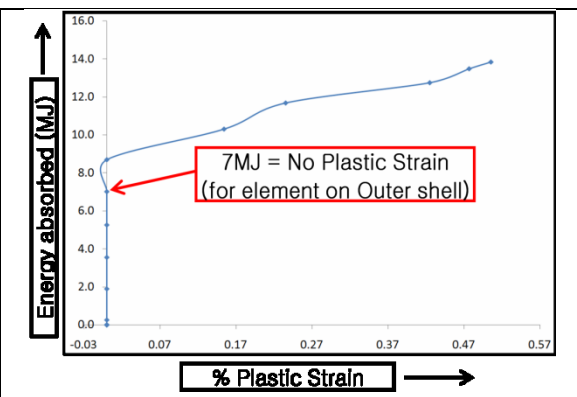
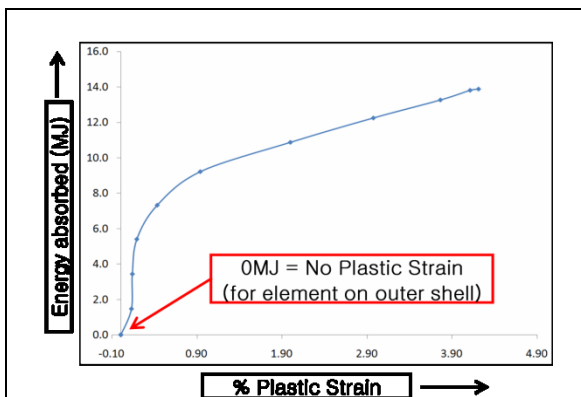


Figure 41. Collision capacity of the outer shell of CPF column for RPF01 (LC01)

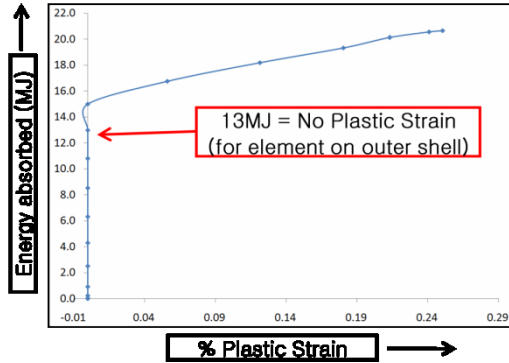


Figure 43. Collision capacity of the outer shell of CPF column for RPF01 (LC03)

Figure 42. Collision capacity of the outer shell of CPF column for RPF01 (LC02)

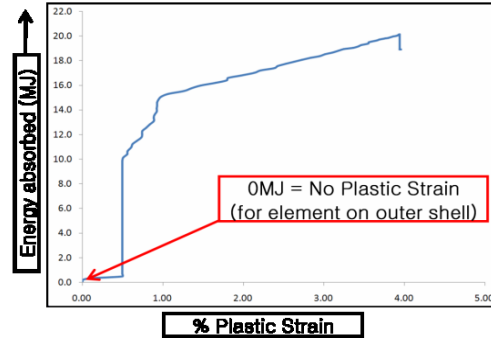


Figure 44. Collision capacity of the outer shell of CPF column for RPF02 (LC01)

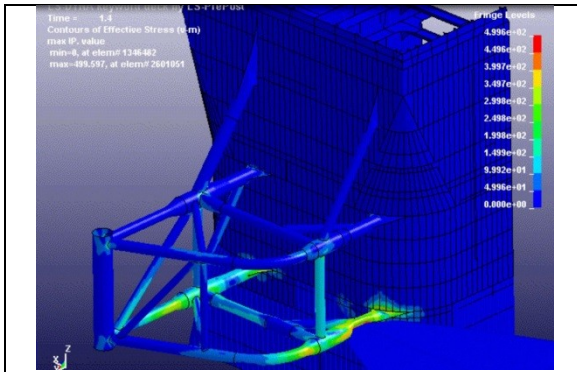


Figure 47. Stress distribution plot of CPF column externals for RPF01 (LC01)

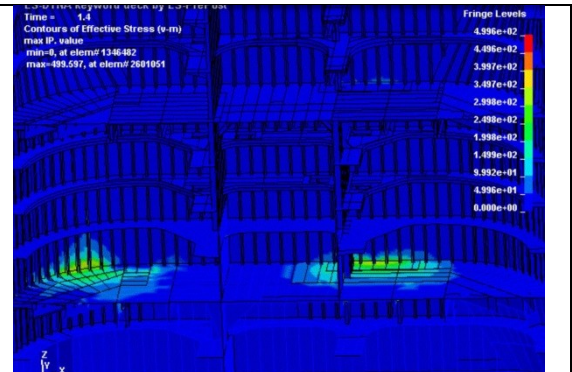


Figure 48. Stress distribution plot of CPF column internals for RPF01 (LC01)

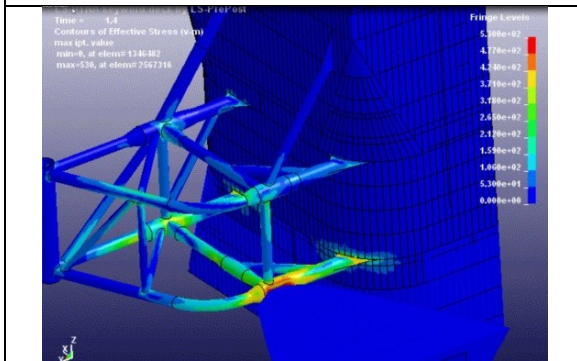


Figure 49. Stress distribution plot of CPF column externals for RPF01 (LC02)

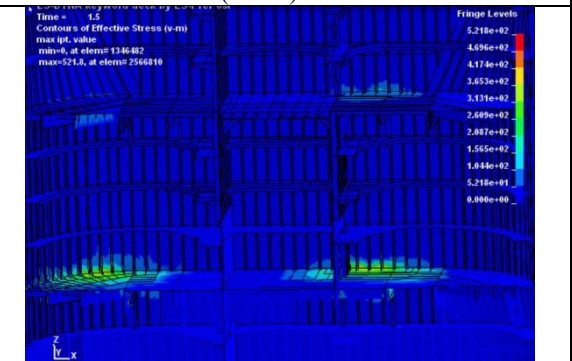


Figure 50. Stress distribution plot of CPF column internals for RPF01 (LC02)

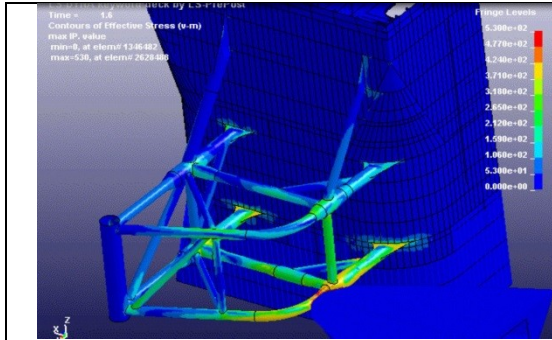


Figure 51. Stress distribution plot of CPF column externals for RPF01 (LC03)

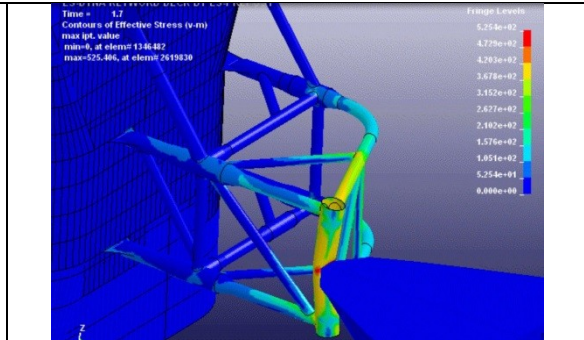


Figure 52. Stress distribution plot of CPF column externals for RPF01 (LC07)

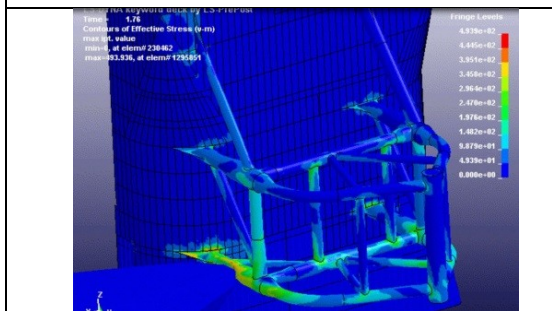


Figure 53. Stress distribution plot of CPF column externals for RPF02 (LC01)

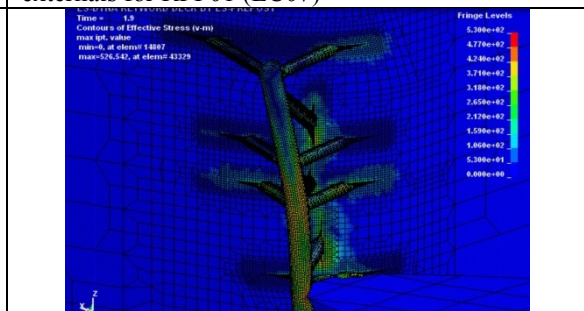


Figure 54. Stress distribution plot of CPF column externals for PN01 (LC01)

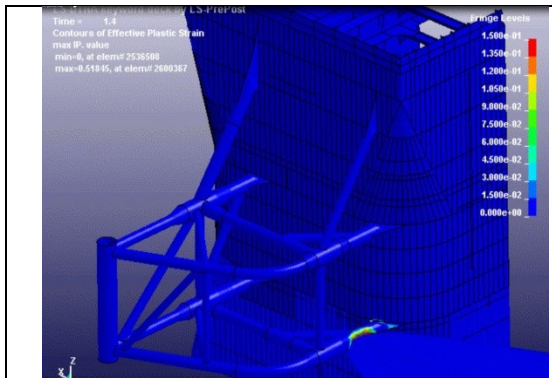


Figure 55. Strain distribution plot of CPF column externals for RPF01 (LC01)

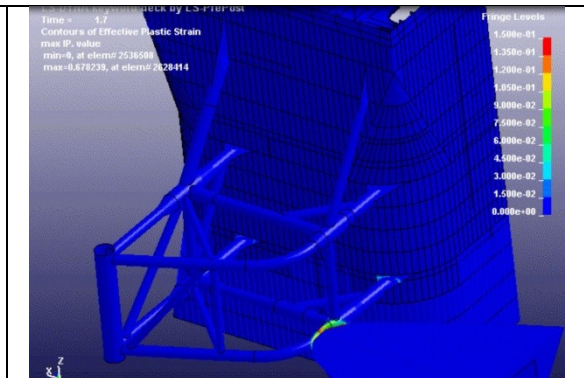


Figure 56. Strain distribution plot of CPF column externals for RPF01 (LC03)

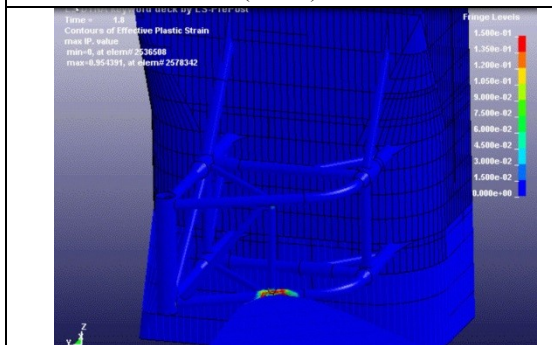


Figure 57. Strain distribution plot of CPF column externals for RPF01 (LC05)

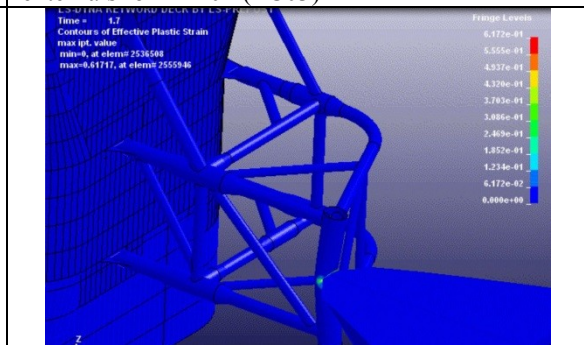


Figure 58. Strain distribution plot of CPF column externals for RPF01 (LC07)

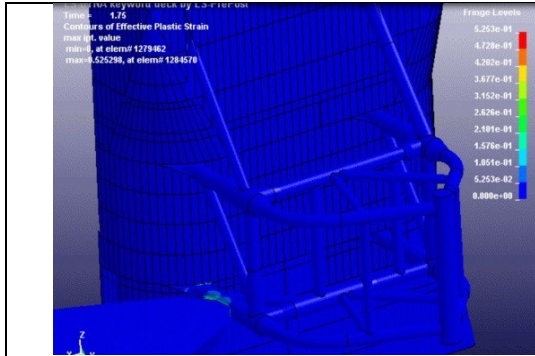


Figure 59. Strain distribution plot of CPF column externals for RPF02 (LC01)

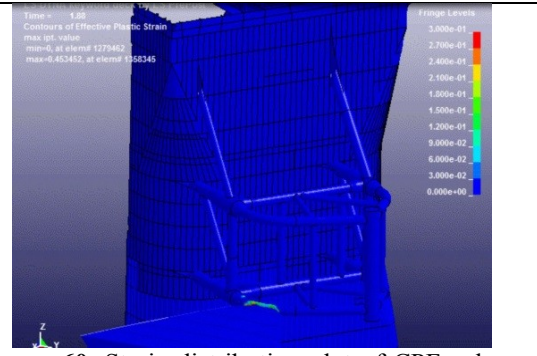


Figure 60. Strain distribution plot of CPF column externals for RPF02 (LC03)

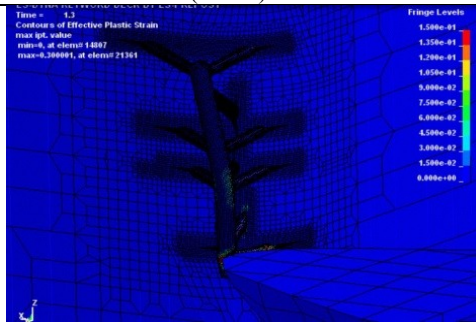


Figure 61. Strain distribution plot of CPF column externals for PN01 (LC02)

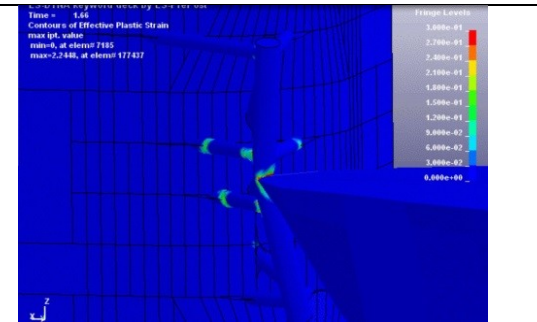


Figure 62. Strain distribution plot of CPF column externals for PN01 (LC05)

6. Conclusion

Collision analysis of the riser protection frame (RPF) and protection net (PN) supports of CPF is performed and presented in this paper.

Initially the collision analysis is performed with an objective of achieving zero plastic strain on the CPF column structure that is supporting the RPF and PN supports but later it is observed that it is very difficult to achieve it. Hence a plastic strain of 5% on the outer shell of the CPF column structure is agreed to be acceptable.

The objective of this analysis is to avoid any kind of leakage into the CPF column due to the collision, so it is important to control the plastic strain on the outer shell of the column. Since the plastic strain of the internal members of the column, RPF and PN structures, doesn't cause any leakage inside the column, there is no criterion for the plastic strain of these structural members.

Thus with the above collision energy and plastic strain criteria, the collision capacities of the RPF and PN supports are estimated along the span of the structures for the given collision energies.

Acknowledgement

The views expressed in this study are this of the author and is not necessarily that of the company with which the author is affiliated.

References

- [1] API Recommended Practice 2A-WSD: Recommended Practice for Planning, Designing and Constructing Fixed Offshore Platforms - Working Stress Design, American Petroleum Institute, 2000.
- [2] Grewal, G. and Lee, M.S., 2004. Strength of minimum structure platforms under ship impact, *Journal of Offshore Mechanics and Arctic Engineering*, pp. 368-375.
- [3] HSE, www.hse.gov.uk, Health and Safety Executive, UK, 2003.
- [4] ISSC, Collision and Grounding. 15th international ship and offshore structures congress, Committee Vol.3, San Diego, USA, 2003.
- [5] ISSC, 16th International ship and offshore structures congress, Vol.2, Committee V.1, Collision and Grounding, Southampton, UK, 20-25 August 2006.
- [6] Lin Y., Feng G., Ren H., and Yu H., 2010. Research on collision strength for deep sea submersible structures, *Proceedings of OMAE*, 20665.
- [7] MMS, MMS OCS spill database, Minerals Management Service, USA, 2000.
- [8] NORSOK Standard, Design of steel structure N-004, Rev.2 October 2004.
- [9] NORSOK Standard, Materials selections M-001, Rev.4 August 2004.
- [10] Oh M., Kim J.H., Jang Y.S. and Bird E., 2005. Impact Analysis of Greater Plutonio FPSO considering ship collision, *International Offshore and Polar Engineering Conference (ISOPE)*; Seoul, Korea.
- [11] Ozguc O., Das P.K., Barltrop N.D.P., 2006. A comparative study on the structural integrity of single and double side skin bulk carriers under collision damage. *Marine Structures*, Vol.18 (7-8). pp. 511-547.

